Available online at www.sciencedirect.com
ScienceDirect
Chinese Journal of Natural Medicines 2020, **18**(2): 114–122
doi: 10.1016/S1875-5364(20)30012-1
Chinese Journal of Natural Medicines

Curcumin-induced cell death depends on the level of autophagic flux in A172 and U87MG human glioblastoma cells

Lee Jong-Eun, Yoon Sung Sik, Lee Jae-Wook, Moon Eun-Yi*

Department of Bioscience and Biotechnology, Sejong University, Seoul 05006, Republic of Korea

Available online 20 Feb., 2020

[ABSTRACT] Glioblastoma is the deadliest neoplasm with the worst 5-year survival rate among all human cancers. Autophagy promotes autophagic cell death or blocks the induction of apoptosis in eukaryotic cells. Here, we investigated whether varying levels of autophagic flux in glioblastoma lead to different efficacies of curcumin treatment using U87MG and A172 human glioblastoma cells. The number of LC3 puncta, the number of cells with LC3 puncta and the level of LC3 II, Atg5 and Atg7 protein were higher in U87MG cells compared with A172 cells. When the cells were incubated with curcumin for 24 or 48 h, the percentage of cell death was higher in A172 cells compared with U87MG cells. Although the level of LC3 was lower, that of curcumin-induced LC3 was higher, in A172 cells than in U87MG cells. The relative increases in cell death and LC3-mediated autophagy were greater under serum starvation in A172 cells compared with U87MG cells. Curcumin-induced A172 cell death was reduced by serum starvation. When both types of cells were transfected with LC3-GFP, the percentage of cell death was higher in A172 cells than that in U87MG cells. Taken together, the data demonstrate that curcumin-mediated tumor cell death is regulated by the basal level of autophagic flux in different glioblastoma cells. This suggests that prior to the use of various curcumin therapeutics, the level of basal or induced autophagic flux should be carefully examined in tumor cells for the best efficacy.

[KEY WORDS] Glioblastoma; A172; U87MG; Autophagic flux; Curcumin
[CLC Number] R965 **[Document code]** A **[Article ID]** 2095-6975(2020)02-0114-09

Introduction

Glioblastoma is among the most aggressive and deadly neoplasms, with the worst 5-year overall survival rate among all human cancers [1-3]. Glioblastoma patients will usually die within 2 years [4-5]. It is therefore necessary to develop new anticancer agents with greater therapeutic potential and lower toxicity profiles [6]. Glioblastomas exhibit overexpression of autophagy-associated proteins at varying levels, which complicates the efficacy of any therapeutic treatment [3].

Autophagy, the process of "self-eating", leads to disassembly of damaged organelles and their recycling for cell survival [7-9]. Stressed cells generate autophagosomes that fuse with lysosomes to form autolysosomes. Autophagosomes are formed by hierarchical recruitment of autophagy-related proteins including Atg5, Atg7, LC3 and Beclin1 to phagophore assembly sites [10]. The autophagy machinery is regulated by molecular mechanisms from transcriptional activation to post-translational modification [7-8, 11]. The contents of the autolysosome are digested by acid hydrolases and recycled into energy sources [8-9, 11].

Many stressful signals sequentially lead to both autophagy and apoptosis within the same cell. Defective autophagy plays a significant role in human pathologies, including cancer, neurodegeneration, and infectious diseases [7]. The connections between autophagy and cell death are complicated [3]. Generally, autophagy inhibits the induction of apoptosis, and apoptosis-associated caspase activation attenuates the autophagic process. However, in many cases, autophagy or autophagy-relevant proteins may support the induction of apoptosis or necrosis, which may result in autophagic cell death (ACD) [8]. Therefore, the relationship between autophagy and ACD has important pathophysiological consequences in the prevention or treatment of disease [8, 12]. However, little is known about the role of autophagic flux in ACD in glioblastoma cells.

Curcumin is the most well-known dietary phytochemical, and it originates from the rhizome of *Curcuma longa* Linn (Zingiberaceae) [13-14]. Curcumin is an antioxidant showing

[Received on] 24-Sep.-2019
[Research funding] This work was supported by the R&D program for Society of the National Research Foundation (NRF) funded by the Ministry of Science, ICT & Future Planning (Grant from Mid-career Researcher Program: No. 2018R1A2A3075602), Republic of Korea.
[*Corresponding author] Tel: 82-2-34083768, Fax: 82-2-4668768, E-mail: eunyimoon@sejong.ac.kr
These authors have no conflict of interest to declare.

various chemotherapeutic effects, such as analgesic, antiseptic, anti-inflammatory, and antimicrobial activities [15-17]. It also has anticancer activities, including tumor initiation, proliferation, progression, metastasis, invasion, and angiogenesis [7, 18]. Control of autophagy by curcumin can regulate its anti-tumor effects [19]. Curcumin-mediated anticancer activity is associated with inhibition of cell growth and induction of apoptosis and autophagy [6, 11, 20-23]. Curcumin can induce autophagy and apoptosis in human gastric cancer cells [14, 23], colon cancer cells [20], brain tumor cells [19], and Sf9 insect cells [21]. Curcumin nanoformulations and targeted forms exhibit enhanced therapeutic efficacy and passage through the blood-brain barrier, compared with natural curcumin [24]. However, the role and involvement of autophagic flux levels have yet to be defined in curcumin-induced cell death.

Therefore, we investigated whether varying levels of autophagic flux in glioblastoma affect the efficacy of curcumin treatment using U87MG and A172 human glioblastoma cells. U87MG and A172 cells have been reported as follows; Acyl-CoA synthetase is an enzyme that produces acyl-CoA by ligation of fatty acid and CoA, and acyl-CoA synthetase 5 is markedly increased in A172 cells but not in U87MG cells [25]. The level of interleukin-1β is higher in U87MG cells than in A172 cells [26]. HER2/neu is positive in A172 cells but not in U87MG cells [27-28]. A172 and U87MG cells are both deficient in the expression of PTEN [29-30] and the DNA repair protein O6-methylguanine-DNA methyltransferase [31]. A172 and U87MG cells express wild-type p53 [26] and Rb [32]. Treatment with TNF-alpha and cisplatin induced apoptosis in U87MG cells but resistance in A172 cells [33]. Curcumin- mediated tumor cell death may be regulated by the autophagic flux level in different glioblastoma cells.

Materials and Methods

Reagents and plasmids

MTT [3(4, 5-dimethyl-thiazol-2-yl)-2, 5-diphenyl tetrazolium bromide], trypan blue solution, and curcumin, were purchased from the Sigma-Aldrich (St. Louis, MO). Antibodies reactive with α-tubulin were obtained from Sigma-Aldrich (St. Louis, MO). Antibodies reactive with LC3-I and II proteins were obtained from NOVUS Biologicals (Littleton, CO). 4', 6-Diamidino-2-phenylindole (DAPI) was purchased from Life Technologies (Grand Island, NY). Except where indicated, all other materials are obtained from Sigma-Aldrich (St. Louis, MO).

pEGFP-C2 plasmid was kindly provided by Prof. Mi-Ock Lee, College of Pharmacy, Seoul National University (Seoul, Rep. of Korea). pGFP-LC3 plasmid was kindly provided by Prof. Dong-Hyung Cho, Graduate School of East-West Medical Science, Kyung Hee University (Yongin, Rep. of Korea).

Cell culture

A172 (CRL-1620) and U87MG (HTB-14) human glioblastoma cell lines were obtained from American Type Cell Culture (ATCC). Cells were maintained and cultured in Dulbecco's modified Eagle's medium supplemented with 10% fetal bovine serum (GIBCO, Grand Island, NY, USA), 2 mmol·L^{-1} L-glutamine, 100 U·mL^{-1} penicillin and 100 U·mL^{-1} streptomycin. Then, cells were incubated at 37 °C in an atmosphere of humidified incubator with 5% CO_2 and 95% air [34-35].

Cytotoxicity assay

Cell survival was quantified by counting cells with trypan blue assay or by using colorimetric assay described for measuring intracellular succinate dehydrogenase content with MTT [36]. Confluent cells were cultured with various concentrations of each reagent for 24 h. Cells were then incubated with 50 μg·mL^{-1} of MTT at 37 °C for 2 h. Formazan formed by MTT were dissolved in dimethylsulfoxide (DMSO). Optical density (*OD*) was read at 540 nm.

FACS analysis

For the analysis of hypodiploid cell formation and each population in cell cycle, cells were fixed in 40% ethanol on ice for 30 min and then incubated with propidium iodide (50 μg·mL^{-1}) and RNase (25 μg·mL^{-1}) at 37 °C for 30 min. Fluorescence intensity of 10 000 cells was analyzed by CELLQuest™ software in FACScalibur™ (Becton Dickinson, San Jose, CA).

Transfection of nucleic acids

Each plasmid DNA was transfected into cells as follows. Briefly, each nucleic acid and lipofectamine 2000 (Invitrogen, Calsbad, CA, USA) were diluted in serum-free medium and incubated for 5 min, respectively. The diluted nucleic acid and lipofectamine 2000 reagent were mixed by inverting and incubated for 20 min to form complexes. In the meanwhile, cells were stabilized by the incubation with culture medium without antibiotics and serum for at least 2 h prior to the transfection. Pre-formed complexes were added directly to the cells and cells were incubated for an additional 6 h. Then, culture medium was replaced with antibiotic and 10% FBS-containing DMEM and incubated for 24–72 h prior to each experiment.

Measurement of autophagy activation

Autophagy was determined by the observation of LC3 puncta-positive structures, which are the essential dynamic process in autophagosome formation [37-38]. Cells were transfected with GFP-LC3 plasmid and treated with curcumin for an appropriate time. Then, cells were fixed with 4% PFA solution freshly prepared in PBS for 10 min. Then, cells were permeabilized with 0.1% Triton X-100 in PBS. Nucleus was visualized by staining cells with DAPI. Then, the number of GFP-LC3 punctas was counted within each sample and autophagic cells were determined by counting the number of cells with GFP-LC3 punctate structure under a fluorescence microscope (Eclipse 80i, Nikon, Japan).

Western blot analysis

Western blotting was performed using a standard protocol. Cells were lysed in ice-cold lysis buffer containing 0.5 % Nonidet P-40 (*V*/*V*) in 20 mmol·L^{-1} Tris-HCl (pH 8.3); 150 mmol·L^{-1} NaCl; protease inhibitors [2 μg·mL^{-1} aprotinin,

pepstatin, and chymostatin; 1 μg·mL^{-1} leupeptin and pepstatin; 1 mmol·L^{-1} phenylmethyl sulfonyl fluoride (PMSF); and 1 mmol·L^{-1} Na_4VO_3]. Lysates were incubated for 1 h on ice before centrifugation at 13 000 r·min^{-1} for 10 min at 4 °C. Protein concentration in each supernatant was measured using a SMART™ BCA protein assay kit (iNtRON Biotech. Inc., Seoul, Republic of Korea). Proteins were denatured by boiling for 5 min in sodium dodecyl sulfate (SDS) sample buffer. Proteins were separated by 12% SDS-polyacrylamide gel electrophoresis (SDS-PAGE), and transferred to nitrocellulose membranes by electro-blotting. Following transfer, equal loading of protein was verified by Ponceau staining. The membranes were blocked with 5% skim milk in Tris-buffered saline with 0.5% Tween 20 (TBST) (10 mmol·L^{-1} Tris-HCl, pH 7.6; 150 mmol·L^{-1} NaCl; 0.5% Tween 20) and incubated with the indicated antibodies. Bound antibodies were visualized with HRP-conjugated secondary antibodies with the use of enhanced chemiluminescence (ECL) (Pierce, Rockford, IL). Primary and HRP-labelled secondary anti-IgG antibodies were diluted 1 : 1000 and 1 : 5000, respectively in TBST. Immunoreactive bands were detected using X-ray film.

Statistical analyses

Experimental differences were tested for statistical significance using ANOVA and Students' *t*-test. *P* values of < 0.05 or < 0.01 were considered to be significant.

Results

Basal levels of autophagic flux differed between A172 and U87MG glioblastoma cells

Malignant glioma is a poor prognosis tumor [6, 19]. Given that U87MG cells are characterized differently from A172 cells [25-32], we examined autophagic flux levels in the two cells. As shown in Fig. 1, autophagic flux levels differed between A172 and U87MG glioblastoma cells. The basal level of autophagic flux was higher in U87MG cells than in A172 cells as determined by the formation of LC3 puncta after transfection of the pGFP-LC3 plasmid (Fig. 1a). The number of autophagic cells with LC3 puncta was also significantly increased in U87MG cells compared with A172 cells (Fig. 1b). The level of LC3 protein was ~5.5 times higher in U87MG cells than in A172 cells (Fig. 1c, left and right). In addition, the level of Atg5 and Atg7 protein was ~2.5 and ~ 1.6 times higher in U87MG cells than in A172 cells, respectively (Fig. 1c, middle and right). Our data suggest that the basal level of autophagic flux might be higher in U87MG cells compared with A172 cells, leading to different responses to the same extracellular signals. It also suggests that the level of LC3 protein is more correlated with the basal level of autophagic flux than Atg5 and Atg7.

Curcumin-induced cell death was inversely associated with the basal level of autophagic flux

Given that glioblastoma has a poor survival rate [6, 19], and

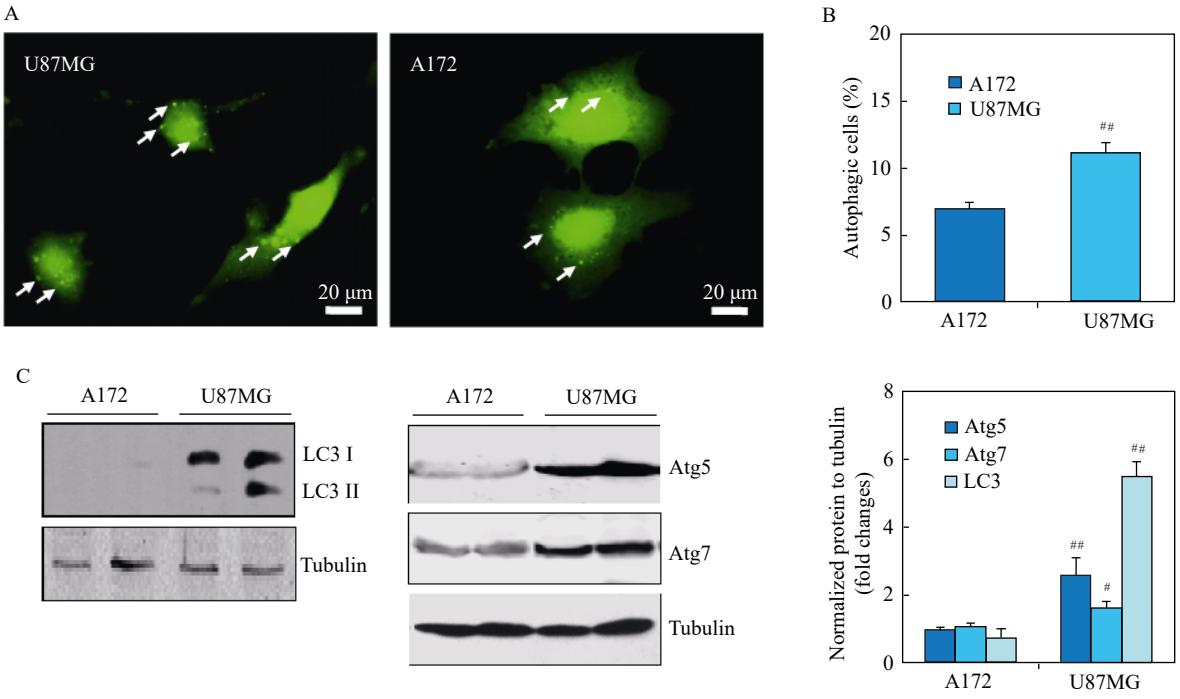

Fig. 1 Autophagy flux level is different in glioblastoma cells. (A–C) A172 and U87MG glioblastoma cells were transfected with pGFP-LC3 plasmids. LC3 puncta in each cell was observed with 1000× magnification under fluorescence microscope. Arrows indicate LC3 puncta (A). Number of cells with LC3 puncta was counted manually (B). Cell lysates were prepared and proteins were analyzed by western blotting. Desity of each band was analyzed by ImageJ 1.34 and results were normalized to tubulin (C). Data were the representative from four experiments. Data in bar graph represent mean ± SED (n = 4). $^{\#}P < 0.05$, $^{\#\#}P < 0.01$ *vs* A172 cells (B and C, right)

that curcumin may induce autophagy and apoptosis in brain tumor cells [19], we evaluated changes in curcumin-induced cell death in U87MG and A172 human glioblastoma cells. As we conducted preliminary experiments with various concentration of curcumin, 10 μmol·L^{-1} curcumin showed the significant changes in autophagy flux and glioblastome cell death (data not shown). Then, MTT assay was performed to assess cell viability in the glioblastoma cells, and showed that U87MG cells (Fig. 2a, left) were more resistant to curcumin-mediated cell death compared with A172 cells (Fig. 2a, right). The cell death rate induced by curcumin treatment was also measured by DAPI staining, which affirmed the results of the MTT assay (Fig. 2b), showing that the cell death rate after 48 h of curcumin treatment was significantly higher in A172 cells than in U87MG cells. Data were confirmed by the measurement of hypodiploid cell formation, which led to apoptotic dead cells with the low fluorescence intensity of propidium iodide (Fig. 2c, left). Hypodiploid cell formation was ~7.5 times and ~2.5 times higher in curcumin-treated A172 and U87MG cells, respectively compared to those in each control cells (Fig. 2c, right). Data demonstrate that curcumin- induced cell death could be higher in A172 cells than that in U87MG cells.

To re-affirm the different effect of curcumin in glioblastoma cells, we examined the changes in each population of cell cycle (Fig. 3a, left). Curcumin-treated cell population was decreased in G_0/G_1 phase but that was increased in G_2/M phase (Fig. 3a, right). Cell population in G_0/G_1 phase was decreased by curcumin treatment to ~38% and ~46% in A172 and U87MG cells, respectively compared to ~59 and 64% in each control cells. Cell population in G_2/M phase was increased by curcumin treatment to ~40% and ~25% in A172 and U87MG cells, respectively compared to ~20% and 19% in each control cells. Next, the LC3 protein level was evaluated by western blot. As shown in Fig. 3b, the level of LC3 protein was higher in U87MG cells (left) than in A172 cells (middle). Whereas U87MG cells showed slight accumulation of LC3 protein by curcumin treatment, A172 cells showed significant accumulation up to ~2.7 and ~2.8 times at 24 or 36 h (right). This suggests that the basal level of autophagic flux may influence the response to curcumin in glioblastoma cells.

Autophagy under serum starvation reduced the cell death rate induced by curcumin

To confirm the effect of autophagic flux on curcumin-induced cell death in glioblastoma cells, cells were serum starved. As shown in Fig. 4, the cell death rate was increased by serum starvation as determined by trypan blue exclusion assay (Fig. 4a). However, little difference in cell death between both cells was observed by serum starvation. The level of LC3 protein was higher in U87MG cells than in

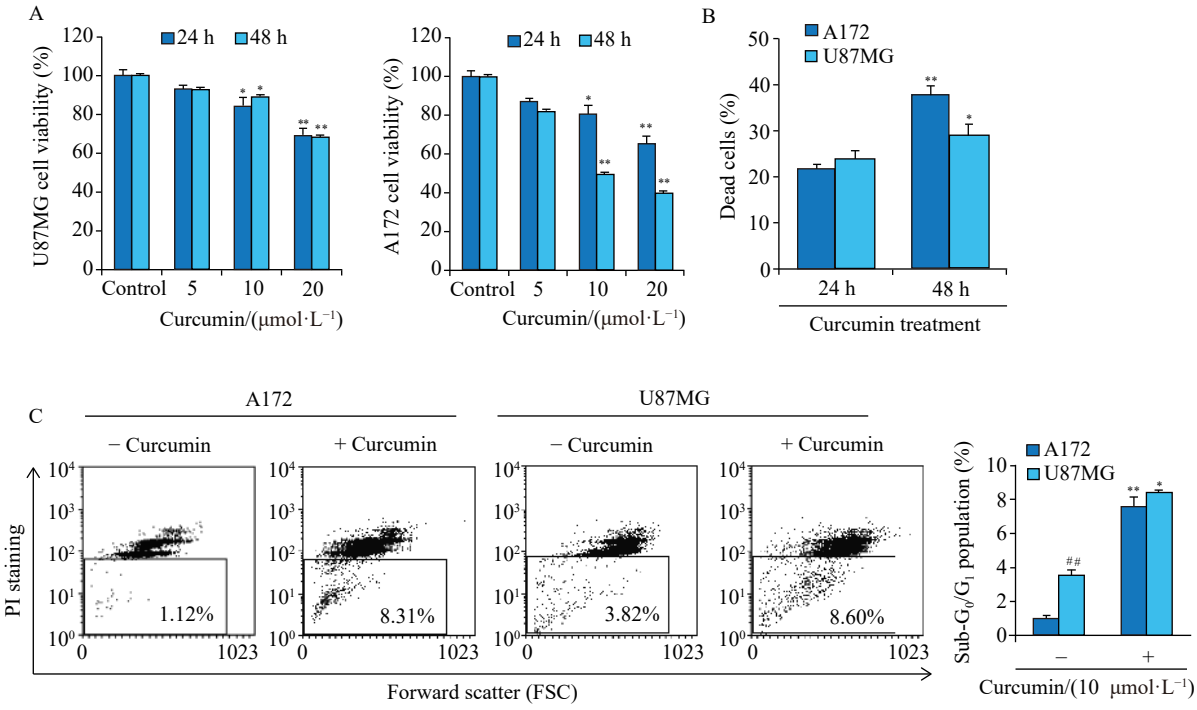

Fig. 2 Cell death rate by curcumin treatment was different in glioblastoma cells. (A) U87MG (left) and A172 (right) glioblastoma cells were treated with 5, 10 and 20 μmol·L^{-1} curcumin for 24 or 48 h. Then, cell viability was determined by the measurement of absorbance with MTT assay. (B) Cells were treated with 10 μmol·L^{-1} curcumin for 24 or 48 h. Then, cells were stained with DAPI and nuclear changes were observed with 400× magnification under fluorescence microscope. Number of dead cells was counted manually. Data were the representative from four experiments (A and B). (C) U87MG and A172 glioblastoma cells were treated with 10 μmol·L^{-1} curcumin for 36 h. Then, cells were fixed with 40% cold ethyl alcohol and stained with propidium iodide. Then, cells were analyzed with flow cytometry. Dot plots for Sub-G_0/G_1 apoptotic population were representative from four experiments. Data in bar graph represent mean ± SED (n = 4). $^{\#\#}P < 0.01$ *vs* A172 cells; $^{*}P < 0.05$; $^{**}P < 0.01$ *vs* the control group of each cell (A, B and C)

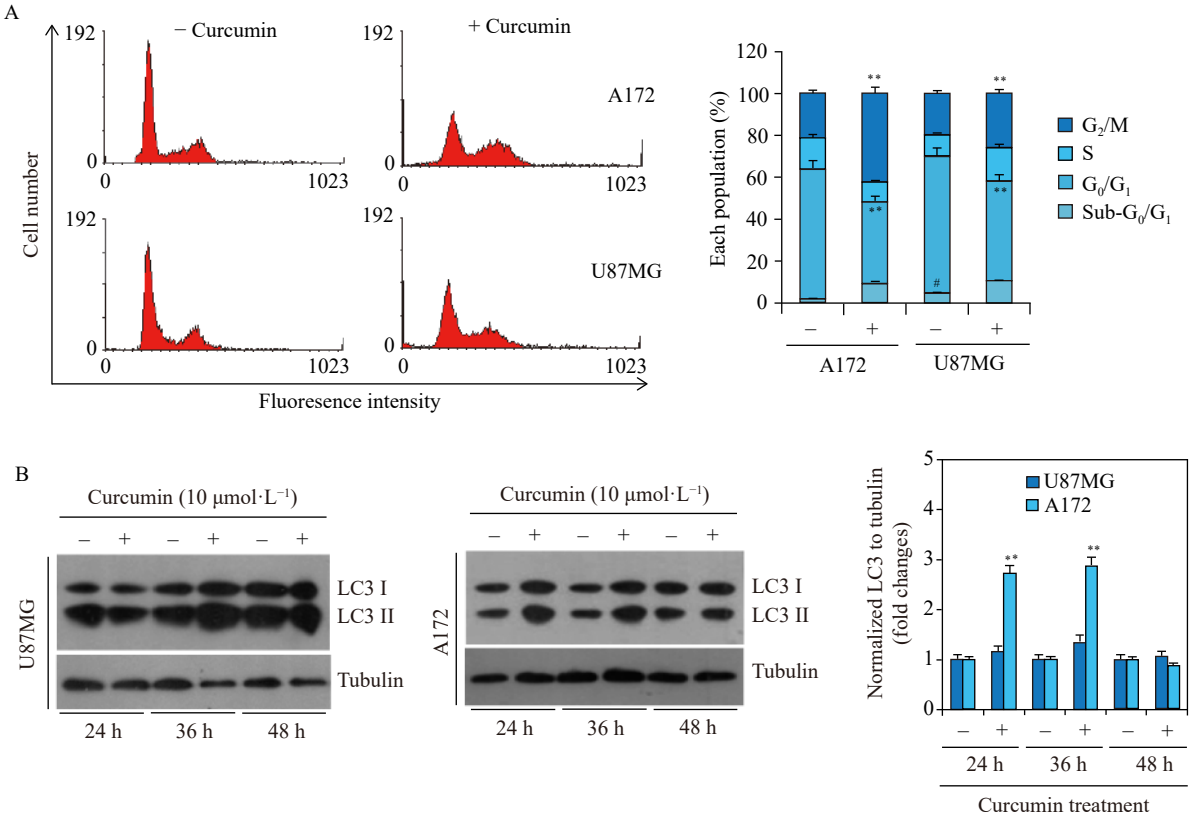

Fig. 3 Cell death by curcumin treatment was compared in glioblastoma cells. (A) U87MG and A172 glioblastoma cells were treated with 10 μmol·L^{-1} curcumin for 36 h. Then, cells were fixed with 40% cold ethyl alcohol and stained with propidium iodide. Then, cells were analyzed with flow cytometry. Histograms for cell cycle were representative from four experiments. (B) Cell lysates were prepared from curcumin-treated U87MG (left) and A172 (right) cells. LC3 proteins were detected by western blotting. Data were the representative from four experiments. Desity of each band was analyzed by ImageJ 1.34 and results were normalized to tubulin. Data in bar graph represent mean ± SED (n = 4). $^{\#}P < 0.05$ *vs* A172 cells; $^{*}P < 0.05$; $^{**}P < 0.01$ *vs* the control group of each cell (A and B)

A172 cells (Fig. 4b). When U87MG and A172 cells were serum starved for up to 6 h, the LC3 protein level was slightly increased in U87MG cells (Fig. 4b, left and right), but significantly increased in A172 cells up to ~7 times (Fig. 4b, middle and right). This result is consistent with the higher number of autophagic cells with LC3 puncta in U87MG control cells than in A172 control cells (Fig. 4c). The percentage of autophagic cells was enhanced by curcumin treatment for 6 h under serum starvation. The relative increase in autophagic cells by curcumin treatment was higher in A172 cells than in U87MG cells (Fig. 4c). When were incubated with curcumin in the presence of 10% FBS, cell death was enhanced significantly. However, the relative increase in cell death by curcumin treatment was lower in A172 cells under serum starvation than in the presence of 10% FBS, as determined by trypan blue exclusion assay and DAPI staining (Fig. 4d). These data suggest that curcumin-induced tumor cell death might be decreased by serum starvation-induced enhancement of autophagic flux levels.

Curcumin-induced cell death was decreased by formation of more LC3 puncta following LC3 overexpression

To confirm the effect of LC3 punctum formation on curcumin-induced cell death, A172 and U87MG cells were transfected with the pEGFP-C2 or pGFP-LC3 plasmid. No LC3 punctum formation was observed in pEGFP-C2-transfected A172 or U87MG cells (Fig. 5a left). By contrast, LC3 punctum formation was higher in U87MG cells than in A172 cells (Fig. 5a right). LC3-GFP proteins in both A172 and U87MG cells were detected by western blot (Fig. 5b). Cell death was higher in A172 cells than in U87MG cells transfected with the pEGFP-C2 or pGFP-LC3 plasmids after treatment with 10 μmol·L^{-1} curcumin for 24 h. Curcumin-induced cell death was increased in both A172 and U87MG cells transfected with the pGFP-LC3 plasmid compared with the respective cells transfected with the pEGFP-C2 plasmid (Fig. 5c). These data suggest that curcumin-induced glioblastoma cell death is decreased by increased LC3 punctum formation.

Discussion

Glioblastoma shows poor outcomes, such as the worst 5-year survival rate of all human cancers, despite multimodal treatments including surgery, chemotherapy, and radiotherapy [1-3, 6, 24]. Glioblastoma overexpresses autophagy-related proteins at varying levels [3]. Generally, autophagy inhibits apoptosis induction, and apoptosis induction inhibits auto-

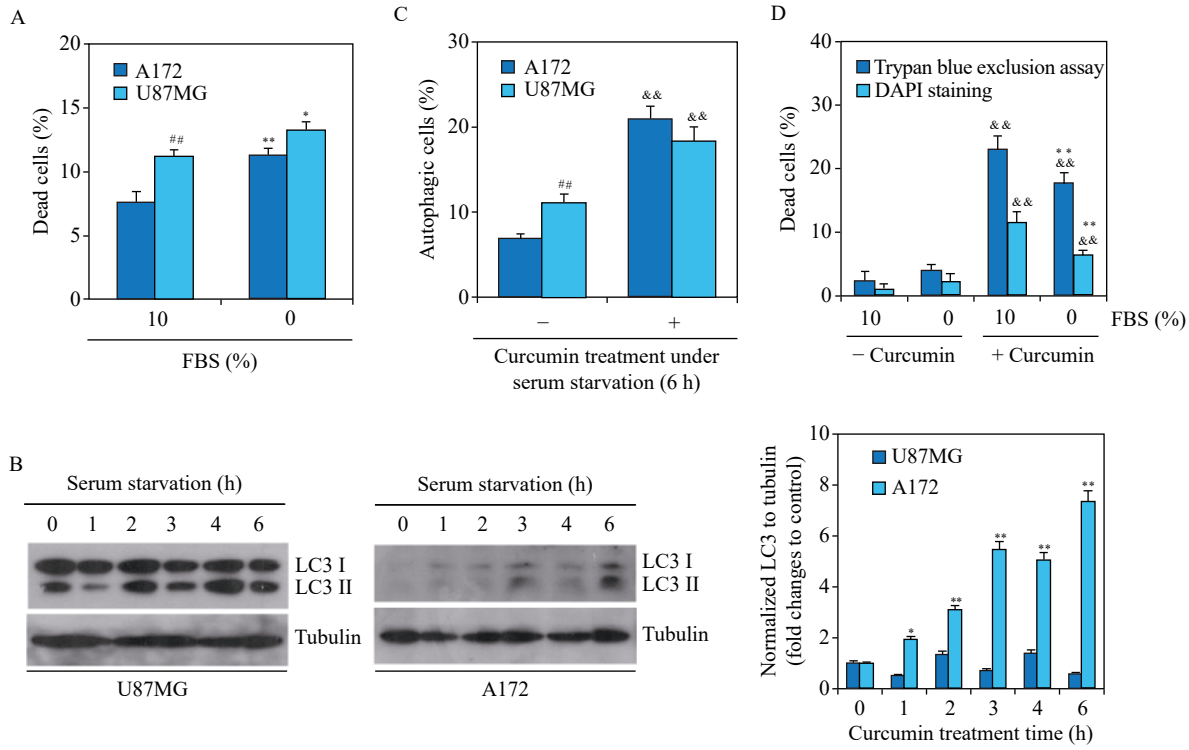

Fig. 4 Cell death rate by curcumin was associated with an increase of autophagy flux level under serum starvation. (A–C) A172 and U87MG glioblastoma cells were incubated in the absence (A, B) or presence (C) of curcumin under serum starvation. Dead cells were estimated by staining them with trypan blue (A). Cell lysates were prepared and LC3 proteins were detected by western blotting. Desity of each band was analyzed by ImageJ 1.34 and results were normalized to tubulin (B). Cells were transfected with pGFP-LC3 plasmids and treated with 10 μmol·L^{-1} curcumin for 6 h under serum starvation. LC3 puncta in each cell was observed with 1000× magnification under fluorescence microscope. Number of cells with LC3 puncta was counted manually (C). (D) A172 cells were incubated with curcumin in the presence of 10 or 0% FBS. Cell death was measured by trypan blue exclusion assay (blue bar) or DAPI staining method (light blue bar). Data were the representative from four experiments. Data in bar graph represent mean ± SED (n = 4) (A, B right, C, D). $^{\#\#}P < 0.01$ *vs* A172 cells; $^{*}P < 0.05$, $^{**}P < 0.01$ *vs* the control group of each cell with 10% FBS (A); $^{\&}P < 0.05$, $^{\&\&}P < 0.01$ *vs* the curcumin-untreated group of each cells (C) or each condition (D)

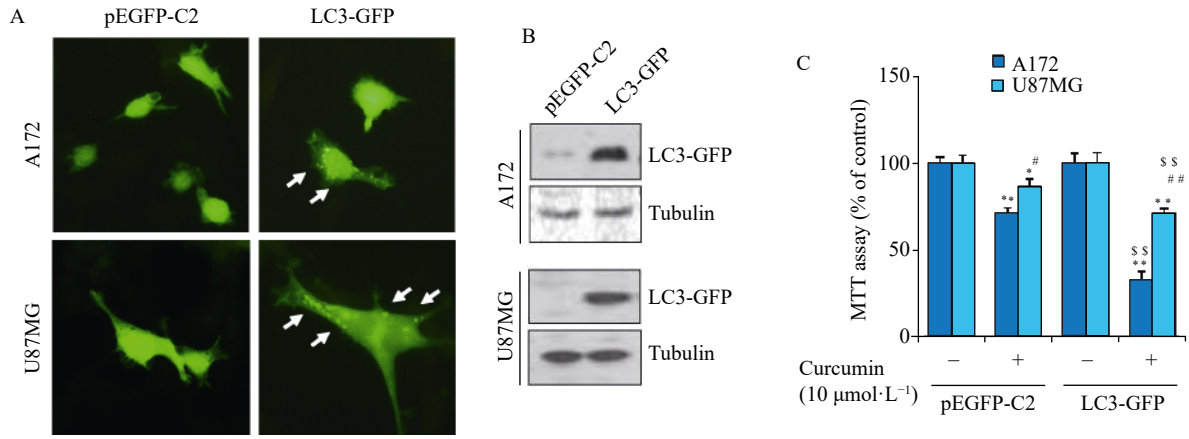

Fig. 5 LC3 overexpression enhanced curcumin-induced cell death. (A–C) A172 and U87MG glioblastoma cells were transfected with pEGFP-C2 or pGFP-LC3 plasmids. LC3 puncta in each cell was observed with 1000× magnification under fluorescence microscope. Arrows indicate LC3 puncta (A). Cell lysates were prepared and LC3-GFP proteins were detected by western blotting (B). Each cell was treated with 10 μmol·L^{-1} curcumin for 24 h. Then, cell viability was determined by the measurement of absorbance with MTT assay. Data were the representative from four experiments. Data in bar graph represent mean ± SED (n = 4). $^{\#}P < 0.05$, $^{\#\#}P < 0.01$ *vs* A172 cells. $^{*}P < 0.05$, $^{**}P < 0.01$ *vs* the curcumin-untreated group of each transfected cell; $^{\$\$}P < 0.01$ *vs* the pEGFP-C2 plasmid-transfected group (C)

phagy. The connections between autophagy and cell death are complicated [3] and have important pathophysiological consequences in the prevention and treatment of disease [8, 12]. It is therefore necessary to develop new therapies with greater therapeutic effects and lower toxicity profiles [6]. Curcumin is the most well-known nutraceutical compound to be evaluated for the treatment of human glioblastoma [6]. However, the role of autophagic flux levels in curcumin-induced cell death has yet to be defined. Here, we investigated whether varying levels of autophagic flux in glioblastoma lead to different efficacies of curcumin treatment using U87MG and A172 human glioblastoma cells. The level of LC3, Atg5 and Atg7 protein was higher in U87MG cells than in A172 cells. Among 3 proteins, the level of LC3 protein is the most different between A172 and U87MG cells. The basal level of autophagic flux might also be higher in U87MG cells than that in A172 cells, which is correlated with LC3 protein more than Atg5 and Atg7. Then, we further studied the effect of curcumin in different glioblastoma cells based on the changes of LC3 protein level. Our data suggest that the effect of curcumin may depend on the autophagic flux level in different glioblastoma cells.

Both autophagy and apoptosis can occur under stress conditions such as serum starvation and anticancer drug treatment [3, 11, 23]. Autophagy and apoptosis are each dominant according to the time and strength of the stimulation. Autophagy inhibits cell death early during the response to stress conditions. As the stress continues, autophagy cannot recover all of the damage to organelles, and cell death is significantly increased [8, 39]. Therefore, anti-tumor drugs become more effective by regulating autophagy early after stress exposure [19].

As curcumin may induce autophagy and apoptosis in various human tumors [14, 19-20, 23], our data suggest that the anti-tumor effect of curcumin is associated with autophagy induced by stress conditions or curcumin in glioblastoma cells (Table 1 and Fig. 6). The autophagic flux level was

Table 1 Relationship between autophagy flux level and curcumin-induced cell death

Cellular condition	Autophagy flux level (AFL)		Curcumin-induced cell death*	
	A172	U87MG	A172	U87MG
Control cells	<		>	
Serum-starved cells	>		≈	
Curcumin-treated cells	>		>	

*When A172 and U87MG glioblastoma cells were incubated with a different condition, curcumin-induced cell death was discriminated by a relative autophagy flux level between both cell types.

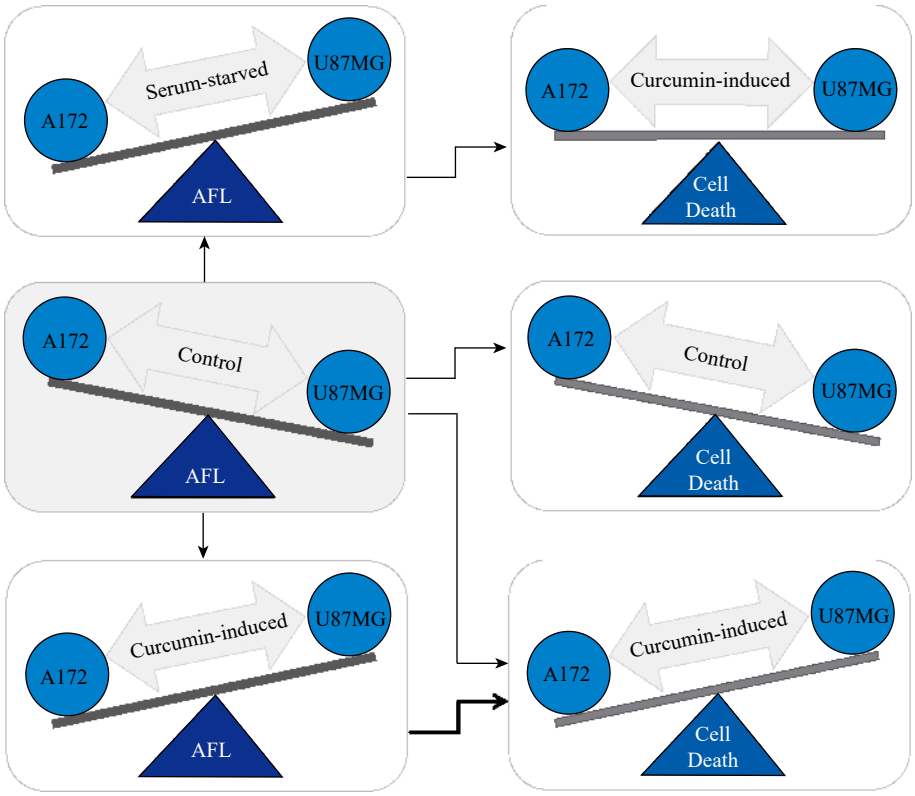

Fig. 6 Scheme for curcumin-induced cell death *via* the changes in autophagy flux level. Curcumin-mediated death in A172 and U87MG glioblastoma cells is associated with autophagy flux level (AFL) pre-existed in each cell or its shift induced by extracellular stimulants such as serum starvation or curcumin itself. Fine lined arrows indicate the changes in AFL and cell death by the application of those various conditions; thick lined arrow indicates the changes in curcumin-mediated AFL and cell death from control cells.

higher in U87MG cells than in A172 cells incubated with 10% FBS. This is consistent with data showing that LC3 punctum formation was higher in U87MG cells than in A172 cells incubated with 10% FBS and transfected with LC3-GFP plasmid DNA. Under these two conditions, curcumin-mediated cell death was lower in U87MG cells than in A172 cells. When both cells types were serum starved, the absolute autophagic flux level was higher in U87MG cells than in A172 cells. However, both the relative increase and the curcumin-induced increase in the autophagic flux level were higher in A172 cells than in U87MG cells. These data suggest that the curcumin-induced autophagic flux level might be attributed more to cell death induced by curcumin than by the pre-existing autophagic flux level or autophagic flux level pre-conditioned by serum starvation or LC3 transfection.

The effect of curcumin is potentiated by G_2/M cell cycle arrest, apoptosis activation, autophagy induction, signaling disturbance, and inhibition of invasion and metastasis [6]. Whereas curcumin upregulates P53 and P21 proteins, it downregulates phosphatidylinositol 3-kinase (PI3K), phosphorylated Akt, and phosphorylated mammalian target of rapamycin (mTOR) [14]. Therefore, the signaling pathway in curcumin-induced cell death may be controlled by PI3K, Akt, and mTOR [3]. Anticancer drug-mediated tumor cell death might also be regulated by signaling molecules such as JNK, Erk, c-myc, and NF-*k*B [40-44]. It is therefore necessary to define the signaling molecules involved in the connection between autophagy and apoptosis induced by curcumin treatment.

Taken together, our findings demonstrate that curcumin's antitumor efficacy on different glioblastoma cells is highly correlated with the balance between its autophagy induction and the pre-existing autophagic flux level. This suggests that autophagy induction may be necessary for optimizing the antitumor activity of curcumin.

References

[1] Tykocki T, Eltayeb M. Ten-year survival in glioblas-toma. A systematic review [J]. *J Clin Neurosci*, 2018, **54**: 7–13.

[2] Pawlowska E, Szczepanska J, Szatkowska M, *et al*. An Interplay between senescence, apoptosis and autophagy in glioblastoma multiforme-role in pathogenesis and therapeutic perspective [J]. *Int J Mol Sci*, 2018, **19**(3): 889.

[3] Lefranc F, Kiss R. Autophagy, the Trojan horse to combat glioblastomas [J]. *Neurosurg Focus*, 2006, **20**(4): E7.

[4] Stupp R, Pavlidis N, Jelic S, *et al*. ESMO Minimum Clinical Recommendations for diagnosis, treatment and follow-up of malignant glioma [J]. *Ann Oncol*, 2005, **16**(Suppl 1): i64–i65.

[5] Verhaak RG, Hoadley KA, Purdom E, *et al*. Integrated genomic analysis identifies clinically relevant subtypes of glioblastoma characterized by abnormalities in PDGFRA, IDH1, EGFR, and NF1 [J]. *Cancer Cell*, 2010, **17**(1): 98–110.

[6] Klinger NV, Mittal S. Therapeutic potential of curcumin for the treatment of brain tumors [J]. *Oxid Med Cell Longev*, 2016, **2016**: 9324085.

[7] Anand P, Nair HB, Sung B, *et al*. Design of curcumin-loaded PLGA nanoparticles formulation with enhanced cellular uptake, and increased bioactivity *in vitro* and superior bioavailability *in vivo* [J]. *Biochem Pharmacol*, 2010, **79**(3): 330–338.

[8] Marino G, Niso-Santano M, Baehrecke EH, *et al*. Self-consumption: the interplay of autophagy and apoptosis [J]. *Nat Rev Mol Cell Biol*, 2014, **15**(2): 81–94.

[9] Monastyrska I, Rieter E, Klionsky DJ, *et al*. Multiple roles of the cytoskeleton in autophagy [J]. *Biol Rev Camb Philos Soc*, 2009, **84**(3): 431–448.

[10] Codogno P, Mehrpour M, Proikas-Cezanne T. Canonical and non-canonical autophagy: variations on a common theme of self-eating? [J]. *Nat Rev Mol Cell Biol*, 2011, **13**(1): 7–12.

[11] Abdul Rahim SA, Dirkse A, Oudin A, *et al*. Regulation of hypoxia-induced autophagy in glioblastoma involves ATG9A [J]. *Br J Cancer*, 2017, **117**(6): 813–825.

[12] Yonekawa T, Thorburn A. Autophagy and cell death [J]. *Essays Biochem*, 2013, **55**: 105–117.

[13] Gupta KK, Bharne SS, Rathinasamy K, *et al*. Dietary antioxidant curcumin inhibits microtubule assembly through tubulin binding [J]. *FEBS J*, 2006, **273**(23): 5320–5332.

[14] Fu HB, Wang CM, Yang DJ, *et al*. Curcumin regulates proliferation, autophagy and apoptosis in gastric cancer cells by affecting PI3K and P53 signaling [J]. *J Cell Physiol*, 2018, **233**(6): 4634–4642.

[15] Wilken R, Veena MS, Wang MB, *et al*. Curcumin: A review of anti-cancer properties and therapeutic activity in head and neck squamous cell carcinoma [J]. *Mol Cancer*, 2011, **10**: 12.

[16] Anand P, Thomas SG, Kunnumakkara AB, *et al*. Biological activities of curcumin and its analogues (Congeners) made by man and Mother Nature [J]. *Biochem Pharmacol*, 2008, **76**(11): 1590–1611.

[17] Sa G, Das T. Anti cancer effects of curcumin: cycle of life and death [J]. *Cell Div*, 2008, **3**: 14.

[18] Kawamori T, Lubet R, Steele VE, *et al*. Chemopreventive effect of curcumin, a naturally occurring anti-inflammatory agent, during the promotion/progression stages of colon cancer [J]. *Cancer Res*, 1999, **59**(3): 597–601.

[19] Zanotto-Filho A, Braganhol E, Klafke K, *et al*. Autophagy inhibition improves the efficacy of curcumin/temozolomide combination therapy in glioblastomas [J]. *Cancer Lett*, 2015, **358**(2): 220–231.

[20] Zhang JB, Wang JG, Xu J, *et al*. Curcumin targets the TFEB-lysosome pathway for induction of autophagy [J]. *Oncotarget*, 2016, **7**(46): 75659–75671.

[21] Veeran S, Shu B, Cui G, *et al*. Curcumin induces autophagic cell death in Spodoptera frugiperda cells [J]. *Pestic Biochem Physiol*, 2017, **139**: 79–86.

[22] Lee JW, Park S, Kim SY, *et al*. Curcumin hampers the antitumor effect of vinblastine *via* the inhibition of microtubule dynamics and mitochondrial membrane potential in HeLa cervical cancer cells [J]. *Phytomedicine*, 2016, **23**(7): 705–713.

[23] Li W, Zhou Y, Yang J, *et al*. Curcumin induces apoptotic cell death and protective autophagy in human gastric cancer cells [J]. *Oncol Rep*, 2017, **37**(6): 3459–3466.

[24] Shahcheraghi SH, Zangui M, Lotfi M, *et al*. Therapeutic potential of curcumin in the treatment of glioblastoma multiforme [J]. *Curr Pharm Des*, 2019, **25**(3): 333–342.

[25] Yamashita Y, Kumabe T, Cho YY, *et al*. Fatty acid in-duced glioma cell growth is mediated by the acyl-CoA synthetase 5 gene located on chromosome 10q25. 1-q25. 2, a region frequently deleted in malignant gliomas [J]. *Oncogene*, 2000, **19**(51): 5919–5925.

[26] Fathima Hurmath K, Ramaswamy P, Nandakumar DN. IL-1beta microenvironment promotes proliferation, migration, and invasion of human glioma cells [J]. *Cell Biol Int*, 2014, **38**(12): 1415–1422.

[27] Mineo JF, Bordron A, Quintin-Roue I, *et al*. Recombinant humanised anti-HER2/neu antibody (Herceptin) induces cellular

death of glioblastomas [J]. *Br J Cancer*, 2004, **91**(6): 1195–1199.
[28] Zhang LM, Ren JL, Zhang HY, *et al*. HER2-targeted recombinant protein immuno-caspase-6 effectively induces apoptosis in HER2-overexpressing GBM cells *in vitro* and *in vivo* [J]. *Oncol Rep*, 2016, **36**(5): 2689–2696.
[29] Shingu T, Yamada K, Hara N, *et al*. Growth inhibition of human malignant glioma cells induced by the PI3-K-specific inhibitor [J]. *J Neurosurg*, 2003, **98**(1): 154–161.
[30] Comelli M, Pretis I, Buso A, *et al*. Mitochondrial energy metabolism and signalling in human glioblastoma cell lines with different PTEN gene status [J]. *J Bioenerg Biomembr*, 2018, **50**(1): 33–52.
[31] Patyka M, Sharifi Z, Petrecca K, *et al*. Sensitivity to PRIMA-1MET is associated with decreased MGMT in human glioblastoma cells and glioblastoma stem cells irrespective of p53 status [J]. *Oncotarget*, 2016, **7**(37): 60245–60269.
[32] Bronner SM, Merrick KA, Murray J, *et al*. Design of a brain-penetrant CDK4/6 inhibitor for glioblastoma [J]. *Bioorg Med Chem Lett*, 2019, **29**(16): 2294–2301.
[33] Duan L, Aoyagi M, Tamaki M, *et al*. Impairment of both apoptotic and cytoprotective signalings in glioma cells resistant to the combined use of cisplatin and tumor necrosis factor alpha [J]. *Clin Cancer Res*, 2004, **10**(1 Pt 1): 234–243.
[34] Lee JW, Ryu YK, Ji YH, *et al*. Hypoxia/reoxygenation-ex-perienced cancer cell migration and metastasis are regulated by Rap1- and Rac1-GTPase activation *via* the expression of thymosin beta-4 [J]. *Oncotarget*, 2015, **6**(12): 9820–9833.
[35] Ryu YK, Lee JW, Moon EY. Thymosin Beta-4, actin-sequestering protein regulates vascular endothelial growth factor expression *via* hypoxia-inducible nitric oxide production in HeLa cervical cancer cells [J]. *Biomol Ther (Seoul)*, 2015, **23**(1): 19–25.
[36] Yang DH, Lee JW, Lee J, *et al*. Dynamic rearrangement of F-actin is required to maintain the antitumor effect of trichostatin A [J]. *PLoS One*, 2014, **9**(5): e97352.
[37] Wu M, Lao YZ, Xu NH, *et al*. Guttiferone K induces autophagy and sensitizes cancer cells to nutrient stress-induced cell death [J]. *Phytomedicine*, 2015, **22**(10): 902–910.
[38] Yao CW, Kang KA, Piao MJ, *et al*. Reduced autophagy in 5-fluorouracil resistant colon cancer cells [J]. *Biomol Ther (Seoul)*, 2017, **25**(3): 315–320.
[39] Cassel M, de Paiva Camargo M, Oliveira de Jesus LW, *et al*. Involution processes of follicular atresia and post-ovulatory complex in a characid fish ovary: a study of apoptosis and autophagy pathways [J]. *J Mol Histol*, 2017, **48**(3): 243–257.
[40] Bressin C, Bourgarel-Rey V, Carre M, *et al*. Decrease in c-Myc activity enhances cancer cell sensitivity to vinblastine [J]. *Anticancer Drugs*, 2006, **17**(2): 181–187.
[41] Calvino E, Tejedor MC, Sancho P, *et al*. JNK and NFkappaB dependence of apoptosis induced by vinblastine in human acute promyelocytic leukaemia cells [J]. *Cell Biochem Funct*, 2015, **33**(4): 211–219.
[42] Fan M, Goodwin M, Vu T, *et al*. Vinblastine-induced phosphorylation of Bcl-2 and Bcl-XL is mediated by JNK and occurs in parallel with inactivation of the Raf-1/MEK/ERK cascade [J]. *J Biol Chem*, 2000, **275**(39): 29980–29985.
[43] Stadheim TA, Xiao H, Eastman A. Inhibition of extracellular signal-regulated kinase (ERK) mediates cell cycle phase independent apoptosis in vinblastine-treated ML-1 cells [J]. *Cancer Res*, 2001, **61**(4): 1533–1540.
[44] Tashiro E, Simizu S, Takada M, *et al*. Caspase-3 activation is not responsible for vinblastine-induced Bcl-2 phosphorylation and G_2/M arrest in human small cell lung carcinoma Ms-1 cells [J]. *Jpn J Cancer Res*, 1998, **89**(9): 940–946.

Cite this article as: Lee Jong-Eun, Yoon Sung Sik, Lee Jae-Wook, Moon Eun-Yi. Curcumin-induced cell death depends on the level of autophagic flux in A172 and U87MG human glioblastoma cells [J]. *Chin J Nat Med*, 2020, **18**(2): 114-122.